Study of the correlation of charge separation of the chiral magnetic effect in Relativistic Heavy-ion Collisions

Sheng-Qin Feng[1,2,3],* Lei Pei[1], Fei Sun[1], Yang Zhong[1], and Zhong-Bao Yin[2]
[1] *College of Science, China Three Gorges UniversityYichang 443002, China*
[2] *Key Laboratory of Quark and Lepton Physics (MOE) and Institute of Particle Physics, Central China Normal University, Wuhan 430079, China and*
[3] *School of Physics and Technology, Wuhan University, Wuhan 430072, China*

It was pointed out that the chiral magnetic effect is a process of charge separation with respect to the reaction plane. There is one kind of phenomenon of gauge field configurations with nonzero topological charge, which can be a sphaleron in the QCD vacuum. At high temperatures, one expects that the sphaleron process is a dominant process. It is believed that a very strong magnetic field can be produced in relativistic heavy-ion collisions, and it is crucial for charge separation. We calculate the chiral separation effects during RHIC and LHC energy regions by studying the detailed chiral charge separation dependencies on the centralities, collision energies and nuclear screening effects in the paper. The response of QGP medium to magnetic field is introduced in the discussion, which help us to study the features of chiral magnetic field and QGP in relativistic heavy-ion collisions.

Keywowds: Chiral magnetic effect, Non-central collision, chiral charge separation the screening effect

PACS numbers: 25.75.Ld, 11.30.Er, 11.30.Rd

arXiv:1609.07550v3 [nucl-th] 28 Sep 2016

I. INTRODUCTION

The characteristic of the quark-gluon plasma(QGP) is studied by QCD, which forecasts that certain special gluon configurations to which one can calculate a winding number in the QGP phase [1–3]. One finds that this winding number is topological invariant, which argues that smooth deformations of these configurations do not change the winding number. Experimental evidence for the existence of configurations with nonzero winding number is only indirect from the meson spectrum [4–6].

The chiral separation effect(CSE) [7] is a similar effect in which the occurrence of a vector charge, e.g. electric charge, causes a separation of chiralities. RHIC [8–12] and LHC [13] have published experimental results of chiral magnetic effect (CME) by particle correlations, which are qualitatively consistent with the CME. Compared with a charge-dependent separation relative to the reaction plane, A clear signal of CSE from LHC energy region [13] shows little or no collision energy dependence when compared to experimental results at RHIC energies. These experimental results [8–13] can help us to study the CSE in relativistic heavy-ion collisions.

In Refs. [14, 15], we improved the magnetic field calculation of the magnetic field for off-central collisions. It is shown that an enormous magnetic field can be produced in off-central relativistic heavy-ion collisions. The huge magnetic field is created just after the collision and then decreases rapidly with time. Numerical magnetic field calculations [14–20] indicate that at RHIC and LHC energies the field strength reaches as large as $B \approx 10^{14}$ T. In a vacuum, the produced magnetic field in the LHC energy region at the initial time is much higher than that of the RHIC region, but decrease with time is much faster than that of in the RHIC region.

Kharzeev, Mclerran and Warringa(KMW) presented new evidence of a charge-parity(CP) violation in relativistic heavy-ion collisions caused by the nonzero Q_w gauge field configurations [19]. KMW proposed that this kind of configuration can separate charge which means the right- and left-hand quarks created during the collisions will move oppositely with respect to the reaction plane in the presence of a background magnetic field. Also, some experiments have obtained a series of results to support the chiral magnetic effect.

In this paper, the detailed studies of CSE in relativistic heavy-ion collisions will be carried out. we will study the dependencies of chiral charge separation on centralities, collision energies and collision nuclei. The paper is organized as follows. The mechanism of CSE will be proposed in Sec. II. The chiral charge separation calculation results are shown in Sec. III. A summary and conclusion is given in Sec. IV.

II. THE MECHANISM OF CHIRAL SEPARATION EFFECT

It was argued out that [19] the chiral magnetic effect (CME) is a process of charge separation with respect to the reaction plane. The charge separation Q is expressed as

*Electronic address: fengsq@ctgu.edu.cn

$$Q \approx 2Q_w \sum_f |q_f|\beta(2|q_f\Phi|), \tag{1}$$

where $\Phi = eB\rho^2$ is the flux through a configuration with non-zero Q_w, Q_w is the topological charge, and $\beta(x)$ related to the microscopic dynamics of quark matter is a function as

$$\beta(x) = \begin{cases} x & for \quad x \leq 1 \\ 1 & for \quad x \geq 1. \end{cases} \tag{2}$$

Now that we studied the ideal situation with an extremely lagre magnetic field eB, and calculated the amount of charge separated in a homogeneous magnetic field with the size ρ of the configuration with non-zero Q_w.

KMW pointed out [19] that if $eB \sim 1/\rho^2$ there is a good probability to get charge separation. The typical required magnetic fields are therefore of order $\alpha_s^2 T^2$, whose magnitude is about $10^2 \sim 10^3$ MeV^2, for the initial conditions typical at RHIC and LHC energy regions. It has been shown that [14–19] such enormous magnetic fields can indeed be created in off-central relativistic heavy-ion collisions. We will take the produced magnetic field in relativistic heavy-ion collisions as a homogeneous magnetic field in the region of overlap of the colliding nuclei in the plasma.

$N_a^{\pm}$ and $N_b^{\pm}$ are denoted as the total positive/negative charge in units of e above(a) and below(b)the reaction plane, respectively. $N^{\pm} = N_a^{\pm} + N_b^{\pm}$ is defined as as the total positive/negative charge produced in a certain event, and $\Delta_{\pm} = N_a^{\pm} - N_b^{\pm}$ is defined to be the difference between on each side of the reaction plane. Each time a transition is made both Δ_+ and Δ_- will change. The expectation value of the change is either positive or negative with equal probability and given by

$$\pm \sum_f |q_f|\beta(2|q_f\Phi|) f_{\pm}(x_{\perp}), \tag{3}$$

where we used the most probable transitions so $Q_w = \pm 1$. The transitions with $Q_w > 1$ are greatly suppressed, so we can ignore it. In order to combine the effect with that transitions near the surface are much more likely to contribute to $\Delta_{\pm}$, we introduce the screening suppression functions $f_{\pm}(x_{\perp})$ as

$$f_{\pm}(x_{\perp}) = \exp(-|y_{\pm}(x) - y|/\lambda), \tag{4}$$

where λ is the screening length and the functions $y_+(x)$ and $y_-(x)$ define the upper and lower y coordinate of the overlap region($y_+(x) = -y_-(x)$). Hence $|y_{\pm}(x) - y|$ is the distance from a point y to the upper/lower part of the surface, and one defines as follows:

$$y_+(x) = \begin{cases} \sqrt{R^2 - (x - b/2)^2} & -R + b/2 \leq x \leq 0 \\ \sqrt{R^2 - (x + b/2)^2} & 0 \leq x \leq R + b/2, \end{cases} \tag{5}$$

where b is the impact parameter and R denotes the radius of the nuclei. We should mention that Eq. (3) is only valid for a constant homogeneous magnetic field. The magnetic field is token as homogeneous field around zero space time rapidity especially for large impact parameters in the overlap region. But the magnetic field has a strong time dependence in the vacuum. In this paper, we will consider the electromagnetic response of the QGP.

Now $N_t^{\pm}$ is denoted as the total number of raising/lowering transitions. Furthermore $N_t = N_t^+ + N_t^-$ is denoted as the total number and Δ_t is denoted as the difference between the number of raising and lowering transitions, i.e., $\Delta_t = N_t^+ - N_t^-$.

The dynamics for Δ_t is exactly governed by a one dimensional random walk we assume that all transitions happen independently from each other. Since there are N_t transitions its variation is proportional to $\sqrt{N_t}$, so that one has

$$< \Delta_t^2 >= \int_{t_i}^{t_f} dt \int_V d^3x \int d\rho \frac{dN_t}{d^3x dt d\rho}, \tag{6}$$

where V denotes the volume in which the transitions occur.

Now we can calculate the variation of $\Delta^{\pm}$. Since we assume that all transitions are independent from each other, the total variation should be the sum of the variation of all contributions. Hence we follow that [19]

$$\begin{aligned} < \Delta_{\pm}^2 > \; &= \; \frac{1}{2} \int_{t_i}^{t_f} dt \int_V d^3x \int d\rho \frac{dN_t}{d^3x dt d\rho} \\ &\times \; [f_-(x_{\perp})^2 + f_+(x_{\perp})^2][\sum_f |q_f|\gamma(2|q_f eB|\rho^2)]^2, \end{aligned} \tag{7}$$

and

$$\begin{aligned} < \Delta_+\Delta_- > \; &= \; -\int_{t_i}^{t_f} dt \int_V d^3x \int d\rho \frac{dN_t}{d^3x dt d\rho} \\ &\times \; [f_-(x_{\perp}) f_+(x_{\perp})][\sum_f |q_f|\gamma(2|q_f eB|\rho^2)]^2. \end{aligned} \tag{8}$$

Using the fact that

$$\rho \sim (\Gamma^{\pm}/\alpha_S)^{-1/4} \sim 1/(\alpha_S T), \tag{9}$$

and the sphaleron transition rate was estimated [19] for QCD to be

$$\frac{dN_t^{\pm}}{d^3x dt} \equiv \Gamma^{\pm} \sim 192.8 \alpha_S^5 T^4. \tag{10}$$

These formulas can be taken as [19]:

$$\begin{aligned} \frac{d < \Delta_{\pm}^2 >}{d\eta} \; &= \; 2\chi\alpha_S [\sum_f q_f^2]^2 \int_{V_{\perp}} d^2x_{\perp} \\ &\times \; [f_-(x_{\perp})^2 + f_+(x_{\perp})^2] \int_{t_i}^{t_f} d\tau \tau [eB(\tau, \eta, x_{\perp})]^2, \end{aligned} \tag{11}$$

and

$$\frac{d<\Delta_+\Delta_->}{d\eta} = -4\chi\alpha_S[\sum_f q_f^2]^2 \int_{V_\perp} d^2x_\perp \times [f_-(x_\perp)f_+(x_\perp)] \int_{t_i}^{t_f} d\tau\tau[eB(\tau,\eta,x_\perp)]^2, \quad (12)$$

where the proper time is $\tau = (t^2 - z^2)^2$ and the space-time rapidity is $\eta = \frac{1}{2}\log[(t + z/(t - z))]$. The volume integral is over the overlap region $V_\perp$ in the transverse plane. The time integral is from the initial time τ_i ($\tau_i = R/\sinh(Y_0)$(Y_0 the beam rapidity) to a final time τ_f. We have assumed here that the magnetic field does not change the sphaleron transition rate dramatically. We have also inserted a constant χ which should be of order one, but with large uncertainties. The detailed expression of the sphaleron transition rate are shown in Ref.[19].

In Refs. [14, 15], we have used the Woods-Saxon nuclear distribution instead of a uniform nuclear distribution [19] to calculate the magnetic fields in relativistic heavy-ion collisions. Two similar relativistic heavy nuclei with charge Z and radius R are traveling in the positive and negative z direction with rapidity Y_0. At $t = 0$ they go through a non-central collision with impact parameter b at the origin point. The center of the two nuclei are taken at $x = \pm b/2$ at time $t = 0$ so that the direction of b lies along the x axis. The region in which the two nuclei overlap contains the participants, the regions in which they do not overlap contain the spectators. As the nuclei are nearly traveling with the speed of light in ultra-relativistic heavy-ion collision experiments, the Lorentz contraction factor γ is so large that the two included nuclei can be taken as pancake shape (as the $z = 0$ plane). The detailed calculation procedure and calculation formula of magnetic field in relativistic heavy-ion collisions can be found in Refs. [14, 15].

We should mention that the electric conductivity σ is not negligible if the produced matter, after a short early-stage evolution, is in the QGP phase. Some publication [20–24] predicted that the QGP can have non-trivial electromagnetic response at high temperature. It is realized that such electromagnetic response will make substantially effect on the time evolution of the electromagnetic fields in the QGP [25–27].

To have an study of the electromagnetic response of QGP, one used the following Maxwells equations [18]:

$$\nabla \times \mathbf{E} = -\frac{\partial \mathbf{B}}{\partial t}, \quad (13)$$

$$\frac{1}{\mu}\nabla \times \mathbf{B} = \epsilon\frac{\partial \mathbf{E}}{\partial t} + \mathbf{J}, \quad (14)$$

where μ and ν are the permeability and permittivity of the QGP, respectively, and are supposed as constants. $\mathbf{J}$ is the electric current given by the Ohms law

$$\mathbf{J} = \sigma(\mathbf{E} + \mathbf{v} \times \mathbf{B}), \quad (15)$$

where $\mathbf{v}$ is the flow velocity of QGP. By Eq.(15), one can take the Maxwell's equations for magnetic field as

$$\frac{\partial \mathbf{B}}{\partial t} = \nabla \times (\mathbf{v} \times \mathbf{B}) + \frac{1}{\sigma\mu}(\nabla^2\mathbf{B} - \mu\varepsilon\frac{\partial^2\mathbf{B}}{\partial t^2}). \quad (16)$$

The first terms are the convection terms and the last terms on the right-hand sides of Eq.(16) are the diffusion terms. The ratio of these two kinds of terms are denoted by the magnetic Reynolds number R_m as

$$R_m = LU\sigma\mu, \quad (17)$$

where U is the characteristic velocity of the flow and L is the characteristic length or time scale of the QGP. By neglecting the diffusion terms (taking $R_m \gg 1$), Ref. [18] toke the ideally conducting limit as

$$\frac{\partial \mathbf{B}}{\partial t} = \nabla \times (\mathbf{v} \times \mathbf{B}). \quad (18)$$

The Bjorken picture for the longitudinal expansion is token as [25, 26]

$$v_z = z/t. \quad (19)$$

The magnetic field can be calculated analytically [18] as

$$B_x(t,x,y,z) = \frac{t_0}{t}e^{-\frac{c_s^2}{2d_y^2}(t^2-t_0^2)}B_x(t_0,x_0,y_0,z_0), \quad (20)$$

and

$$B_y(t,x,y,z) = \frac{t_0}{t}e^{-\frac{c_s^2}{2d_x^2}(t^2-t_0^2)}B_y(t_0,x_0,y_0,z_0). \quad (21)$$

where $\mathbf{B}^0(\mathbf{r}) = \mathbf{B}(t = t_0, \mathbf{r})$ (t_0 the formation time of the QGP), c_s is the speed of sound, and $d_{x,y}$ are the root-mean-square widths of the transverse distribution.

From Above, we can see that the evolution of $\mathbf{B}$ is strongly influenced by its initial spatial distribution. However, the time evolution of the magnetic fields at the central region **r=0**, takes very simple forms as

$$B_x(t,\mathbf{0}) = \frac{t_0}{t}e^{-\frac{c_s^2}{2d_y^2}(t^2-t_0^2)}B_x^0(\mathbf{0}), \quad (22)$$

and

$$B_y(t,\mathbf{0}) = \frac{t_0}{t}e^{-\frac{c_s^2}{2d_y^2}(t^2-t_0^2)}B_y^0(\mathbf{0}). \quad (23)$$

In Eqs.(22) and (23), we set $d_x \sim d_y \sim 3$ and $c_s^2 \sim 1/3$. In Refs.[13, 14], we calculated the dependencies of magnetic field eB in the vacuum (at central point $(x, y) = (0, 0)$) on proper time τ at $\sqrt{s_{NN}} = 200$ GeV for Au - Au collisions with b = 8 fm and $\sqrt{s_{NN}} = 2760$ GeV for

Pb - Pb collisions with b = 8 fm, respectively. In this paper, we study the dependencies of magnetic field eB on proper time τ by considering response of QGP medium.

Fig. 1(a, b) show the dependencies of magnetic field eB_y (at central point $(x, y) = (0, 0)$)on proper time τ at $\sqrt{s_{NN}} = 2760$ GeV(a) for Pb-Pb collisions and 200 GeV(b) for Au-Au collisions with b = 8 fm, respectively. The solid line and dashed line are for the consideration of response of QGP medium and in the vacuum with no consideration of response of QGP medium,respectively. It is found that magnetic field with the consideration of response of QGP medium decrease more slowly than that of in the vacuum which has no response of QGP medium. This means that, after considering the QGP response, the magnetic field will last much longer.

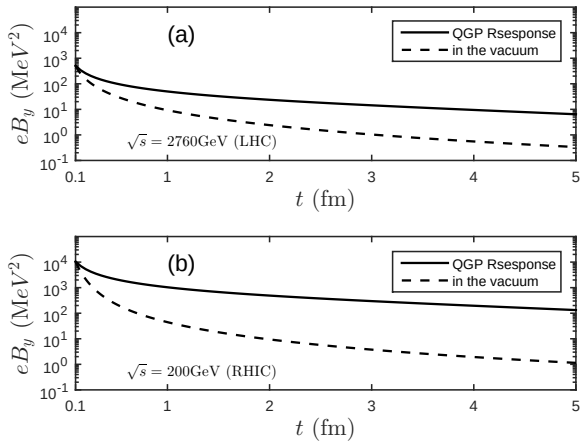

FIG. 1: The dependencies of magnetic field eB_y (at central point $(x, y) = (0, 0)$)on proper time τ at $\sqrt{s_{NN}} = 2760$ GeV(a) for Pb-Pb collisions and 200 GeV(b) for Au-Au collisions with b = 8 fm, respectively. The solid line and dashed line are for the consideration of response of QGP medium and in the vacuum with no response of QGP medium, respectively.

III. THE CALCULATIONS OF CHIRAL CHARGE SEPARATION

A set of very useful correlators for the study of charge separation was proposed by Voloshin [27]. For each event, one defines [19, 27]

$$g(\phi_s, \phi_t) = \frac{1}{N_s N_t} \sum_{i=0}^{N_s} \sum_{i=0}^{N_t} \cos(\phi_{si} + \phi_{ti}), \tag{24}$$

where $s, t = \pm$ denotes the charge sign, ϕ_{si} denotes the azimuthal angle of an individual charged particle with respect to the reaction plane, and $N_\pm$ is the total number of positively or negatively charged particle.

Then one can average the correlators over N_e similar events to remove the multiplicity fluctuations. This averaging is called event mixing. One can define the averaged correlators a_{++}, a_{--}, a_{+-} and a_{-+} [19, 26] as

$$a_{st} = -\frac{1}{N_e} \sum_{n=1}^{N_e} g(\phi_s, \phi_t). \tag{25}$$

The correlators can also be given as

$$g(\phi_s, \phi_t) = \frac{1}{N_s N_t}(X_s X_t - Y_s Y_t), \tag{26}$$

where

$$X_\pm \equiv \sum_{i=1}^{N_\pm} \cos(\phi_i^\pm), \qquad Y_\pm \equiv \sum_{i=1}^{N_\pm} \sin(\phi_i^\pm) \tag{27}$$

If all charged particles would be really emitted perpendicular to the reaction plane in which case $\phi = \pi/2$ or $\phi = 3\pi/2$, we will have

$$Y_\pm = \Delta_\pm. \tag{28}$$

As a result, we would have

$$a_{++} = a_{--} = \frac{1}{N_+^2} < \Delta_\pm^2 >, \tag{29}$$

and

$$a_{+-} = a_{-+} = \frac{1}{N_+ N_-} < \Delta_+ \Delta_- >, \tag{30}$$

where $N_\pm$ denotes the total number of charged particles in the related η interval.

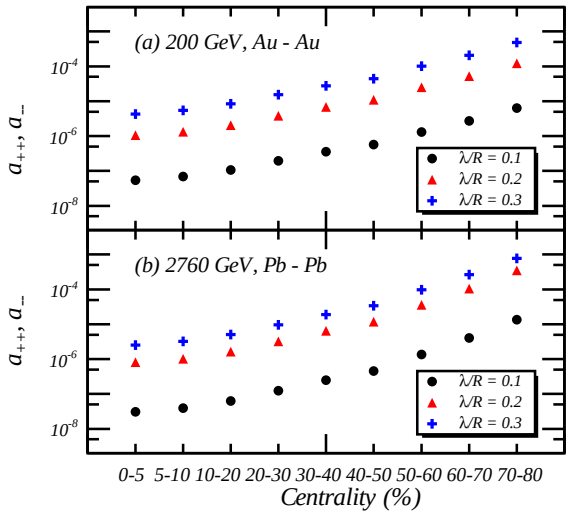

FIG. 2: $a_{++}(a_{--})$ of the CME as a function of centrality for Au - Au collisions at $\sqrt{s_{NN}} = 200$ GeV(a) of RHIC energy region, and for Pb - Pb collisions at $\sqrt{s_{NN}} = 2760$ GeV(b) of LHC energy region for different values of the screening length λ.

Refs. [28, 29] published some geometrical properties of the collision, such as the number of participating nucleons and the number of binary nucleon-nucleon collisions,

which are deduced from a Glauber model with a sharp impact parameter selection and shown to be consistent with those extracted from the data of RHIC and LHC energy regions. Figure 2(a, b) show the dependencies $a_{++}(a_{--})$ of the chiral magnetic effect as a function of centrality, for Au - Au collisions at $\sqrt{s_{NN}} = 200$ GeV(a) of RHIC energy region, and for Pb - Pb collisions at $\sqrt{s_{NN}} = 2760$ GeV(b) of LHC energy region for different values of the screening length $\lambda = 0.1$R, 0.2R and 0.3R, respectively. One find that $a_{++}(a_{--})$ increases with the increase of centralities. One also find that $a_{++}(a_{--})$ increases with the increase of nuclear screening length. Our result for a_{++} and a_{+-} is displayed in Fig. 2. Qualitatively the result agrees with the data presented in Ref. [30, 31].

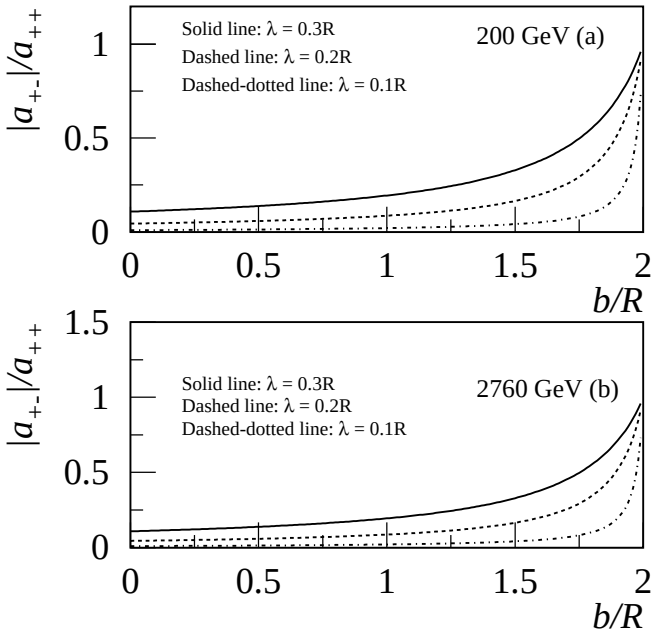

FIG. 3: The result of the correlator $|a_{+-}|/a_{++}$ as a function of b/R for Au - Au collisions at $\sqrt{s_{NN}} = 200$ GeV (a) of RHIC energy region, and for Pb - Pb collisions at $\sqrt{s_{NN}} = 2760$ GeV (b) of LHC energy region for different values of the screening length λ.

We showed $|a_{+-}|/a_{++}$ as a function of b/R in Fig.3 for different values of λ. To calculate the functions a_{+-} and a_{++} we used the screening suppression factor $f_{\pm}(x_{\perp})$ given in Eq.(4). It is found that the suppression of a_{+-} compared to a_{++} decreases with the increase of impact parameter. This is because the system size is smaller in larger impact parameter.

We make a comparison of $a_{++}(a_{--})$ of the chiral magnetic effect as a function of centralities with different screening length between Au - Au collisions at $\sqrt{s_{NN}} = 200$ GeV and that of Cu - Cu collisions in Fig.4(a). One finds that the smaller the collision system, the larger the $a_{++}(a_{--})$ is. We also make a comparison of $|a_{+-}|/a_{++}$ of the chiral magnetic effect as a function of centralities with different screening length between Au - Au collisions

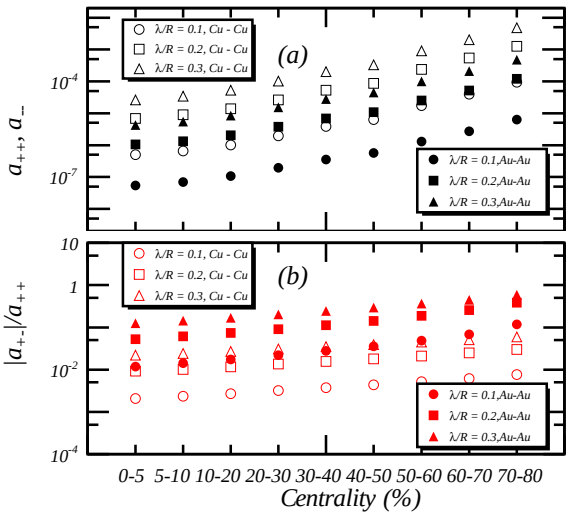

FIG. 4: Comparison of $a_{++}(a_{--})$(a) of the chiral magnetic effect as a function of centralities with different screening length between Au - Au collisions and that of Cu - Cu collisions at $\sqrt{s_{NN}} = 200$ GeV. Comparison of $|a_{+-}|/a_{++}$ (b) of the chiral magnetic effect as a function of centralities with different screening length between Au - Au collisions and that of Cu - Cu collisions at $\sqrt{s_{NN}} = 200$ GeV.

at $\sqrt{s_{NN}} = 200$ GeV and that of Cu - Cu collisions in Fig.4(b). It is found that $|a_{+-}|/a_{++}$ of larger Au - Au collision system is larger than that of smaller Cu - Cu collision system.

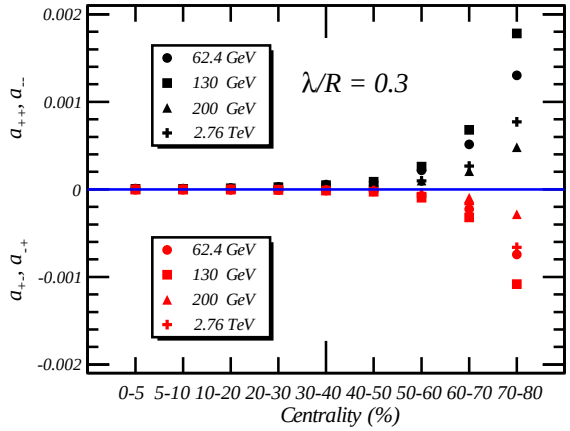

FIG. 5: $a_{++}(a_{--})$(a) and $a_{+-}(a_{-+})$(b) of the chiral magnetic effect as a function of centralities for different collision energies at $\sqrt{s_{NN}} = 62.4$ GeV, 130GeV, 200GeV and 2760 GeV of RHIC and LHC energy regions for the screening length $\lambda/R = 0.3$.

Fig.5 shows the dependencies of $a_{++}(a_{--})$(a) and $a_{+-}(a_{-+})$(b) on the centralities with different collision energies of $\sqrt{s_{NN}} = 62.4$ GeV, 130GeV, 200GeV and 2760 GeV in the RHIC and LHC energy regions for the

screening length $\lambda/R = 0.3$. It is found that the chiral separation effect increases with the impact parameter increases. The chiral separation effect approaches zero at central collisions and the maximum value of the chiral separation effect can reach 1.8×10^{-3} when the screening length $\lambda/R = 0.3$.

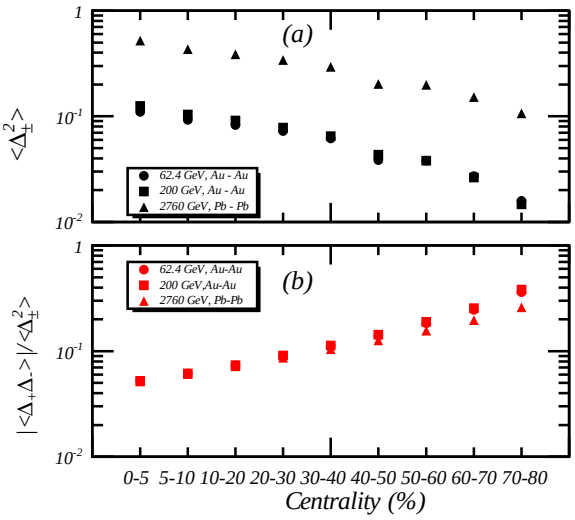

FIG. 6: $< \Delta_{\pm}^2 >$(a) and $< \Delta_+\Delta_- > / < \Delta_{\pm}^2 >$ (b) of the chiral magnetic effect as a function of centralities for different collision energies at $\sqrt{s_{NN}}$ = 62.4 GeV, 200GeV and 2760 GeV of RHIC and LHC energy regions for the screening length $\lambda/R = 0.2$.

Fig.6(a) shows the dependencies of $< \Delta_{\pm}^2 >$ of the chiral magnetic effect as a function of centralities for different collision energies at $\sqrt{s_{NN}}$ = 62.4 GeV, 200GeV and 2760 GeV of RHIC and LHC energy regions. It is found that $< \Delta_{\pm}^2 >$ is larger at LHC energy region $\sqrt{s_{NN}}$ = 2760 GeV than that RHIC energy region $\sqrt{s_{NN}}$ = 62.4 GeV and 200GeV , and the $< \Delta_{\pm}^2 >$ is almost the same in the RHIC energy region.

Fig.6(b) shows the dependencies of $< \Delta_+\Delta_- > / < \Delta_{\pm}^2 >$ of the chiral magnetic effect as a function of centralities for different collision energies at $\sqrt{s_{NN}}$ = 62.4 GeV, 200GeV and 2760 GeV of RHIC and LHC energy regions. It is found that $< \Delta_{\pm}^2 >$ is larger at that $\sqrt{s_{NN}}$ = 2760 GeV of LHC energy region than that of $\sqrt{s_{NN}}$ = 62.4 GeV and 200GeV of RHIC energy region, and the $< \Delta_{\pm}^2 >$ at $\sqrt{s_{NN}}$ = 62.4 GeV and 200GeV in the RHIC energy region is almost the same.

IV. SUMMARY AND CONCLUSION

In this paper, we study systematically the dependencies of chiral charge separation on centralities, collision energies and collision nuclei in the RHIC and LHC energy regions. The response of QGP medium to magnetic field is introduced in the discussion, which help us to study the features of chiral magnetic field and QGP in relativistic heavy-ion collisions. Recent years lots of the research of parity violation in the strong interaction using relativistic heavy-ion collisions has been carried out. It is believed that this symmetry violation originates from the interaction between quarks and topologically nontrivial gluonic fields and sphalerons. This interaction characterized by the topological charge breaks the balance between the number of quarks with different chirality, and creates a violation of the P and CP symmetry.

The dependencies a_{++} of the chiral magnetic effect as a function of centrality, for Au - Au collisions at $\sqrt{s_{NN}}$ = 200 GeV of RHIC energy region, and for Pb - Pb collisions at $\sqrt{s_{NN}}$ = 2760 GeV of LHC energy region for different values of the screening length λ are given in this paper. It is found that a_{++} increases with the increase of impact parameter and nuclear screening length. Qualitatively the result agrees with the data presented in Ref. [30, 31]. It is found that nuclear screening effect has an important influence on the chiral separation characteristics.

We make a comparison between $a_{++}(a_{--})$ of the chiral magnetic effect as a function of centralities with different screening length of Au - Au collisions at $\sqrt{s_{NN}}$ = 200 GeV and that of Cu - Cu collisions. It is shown that the smaller the collision system, the larger the $a_{++}(a_{--})$ is. We also make a comparison between $|a_{+-}|/a_{++}$ of the chiral magnetic effect as a function of centralities with different screening length of Au - Au collisions at $\sqrt{s_{NN}}$ = 200 GeV and that of Cu - Cu collisions. It is found that $|a_{+-}|/a_{++}$ of the larger Au - Au collision system is larger than that of smaller Cu - Cu collision system.

We also find that the chiral separation effect increases with the impact parameter increases. The chiral separation effect approaches zero at central collisions and the maximum value of the chiral separation effect can reach 1.8×10^{-3} when the screening length $\lambda/R = 0.3$ in the RHIC and LHC energy regions.

V. ACKNOWLEDGMENTS

This work was supported by National Natural Science Foundation of China (Grant Nos: 11475068, 11247021, 11447023), the CCNU-QLPL Innovation Fund (Grant No: QLPL2014P01), the Excellent Youth Foundation of Hubei Scientific Committee (Grant No: 2006ABB036).

[1] G. t Hooft, Phys. Rev. Lett. 37, 8 (1976); Phys. Rev. D 14, 3432 (1976).
[2] A. A. Belavin, A. M. Polyakov, A. S. Shvarts, and Yu. S. Tyupkin, Phys. Lett. 59B, 85 (1975).
[3] J.-H. Gao, Z.-T. Liang, S. Pu, Q. Wang, and X.-N. Wang, Phys. Rev. Lett. 109, 232301(2012)
[4] E. Witten, Nucl. Phys. B156, 269 (1979); G. Veneziano, Nucl. Phys. B159, 213 (1979).
[5] G. t Hooft, Phys. Rep. 142, 357 (1986).
[6] M. C. Chu, J. M. Grandy, S. Huang, and J.W. Negele, Phys. Rev. D 49, 6039 (1994); C. Michael and P. S. Spencer, Phys. Rev. D 52, 4691 (1995).
[7] K. Fukushima, D. Kharzeev, and H. J. Warringa, Phys.Rev. D 78, 074033 (2008); L.G. Pang, Q. Wang, and X.-N. Wang, Phys. Rev. C 86, 024911(2012).
[8] Abelev B I, Aggarwal M M, Ahammed Z et al.(STAR Collaboration), Phys. Rev. Lett. 103, 251601 (2009).
[9] Abelev B I, Aggarwal M M, Ahammed Z et al.(STAR Collaboration), Phys. Rev. C 81, 054908 (2010)
[10] Selyuzhenkov I V, (STAR Collaboration), Romanian Reports in Physics, 58, 49 (2006)
[11] S. A. Voloshin, Nucl. Phys. A 830, 377(2009)
[12] Ajitanand N N, Lacey R A, Taranenko A, Alexander J M et al.(STAR Collaboration) Phys. Rev. C 83, 011901 (2011).
[13] Abelev B I, Adam J, Adamova D et al.(ALICE Collaboration), Phys. Rev. Lett., 110, 012301(2013).
[14] Y. J. Mo, S. Q. Feng, and Y. F. Shi, Phys. Rev. C 88, 024901(2013).
[15] Y. Zhong, C.-B. Yang, X. Cai, and S.-Q. Feng, Adv.High Energy Phys. 2014, 193039(2014); Y. Zhong, C.-B. Yang, X. Cai, and S.-Q. Feng, Chinese Physics C 39, 104105 (2015).
[16] V. Voronyuk, V. D. Toneev, W. Cassing, E. L. Bratkovskaya, V. P. Konchakovski, and S. A. Voloshin, Phys. Rev. C 83, 054911 (2011).
[17] V. Skokov, A. Y. Illarionov, and V. Toneev, Int. J. Mod. Phys. A24, 5925 (2009).
[18] W. T. Deng, and X. G. Huang, Phys. Rev. C 85, 044907 (2012); W. T. Deng, and X. G. Huang, Phys.Rev. C93 064907 (2016).
[19] D. E. Kharzeev, L. D. McLerran , H. J. Warringa, Nucl. Phys. A 803, 227 (2008).
[20] P. B. Arnold, G. D. Moore, and L. G. Yaffe, J. High Energy Phys. 05 (2003) 051; L.G. Pang, Gergely Endrödi , H. Petersen, Phys.Rev. C 93 044919(2016).
[21] S. Gupta, Phys. Lett. B 597, 57 (2004).
[22] G. Aarts, C. Allton, J. Foley, S. Hands, and S. Kim, Phys. Rev.Lett. 99, 022002 (2007);
[23] H. T. Ding, A. Francis, O. Kaczmarek, F. Karsch, E. Laermann,and W. Soeldner, Phys. Rev. D 83, 034504 (2011).
[24] A. Francis and O. Kaczmarek, Prog.Part.Nucl.Phys. 67, 212 (2012).
[25] S. F. Taghavi and U. A. Wiedemann, Phys. Rev. C 91, 024902 (2015).
[26] J. Y. Ollitrault, Eur. J. Phys. 29, 275 (2008).
[27] S.A. Voloshin, Phys. Rev. C 70 (2004) 057901.
[28] B. I. Abelev et al.(ALICE Collaboration), Phys. Rev. C 88, 044909(2013).
[29] B. I. Abelev et al.(STAR Collaboration), Phys. Rev. C 79, 034909 (2009).
[30] L. Adamczyk et al.(STAR Collaboration),Phys. Rev. Lett. 114, 252302 (2015); B. I. Abelev et al.(ALICE Collaboration), Phys. Rev. Lett. 110, 012301 (2013).
[31] B. I. Abelev et al.(STAR Collaboration), Phys. Rev. Lett. 103, 251601 (2009); B. I. Abelev et al.(STAR Collaboration),Phys. Rev. C 81, 054908 (2010).